As originally published in the SMTA Proceedings.

Conformal Coating Testing in Various Test Environments

P. Singh[1], L. Palmer[1], C. Xu[2], J. Kaufman[2], H. Fu[3], S. Strixner[4], H. Schweigart[4], M. R. Meier[4], C. Wang[5], M. Pudas[6], M Smith[7], J. Payne[7], H. Remore[7], M. Zhai[8], S. Calvelli[8,9], H. Shi [8], A. Locquet[8], D. S. Citrin[8], D. Hampannavar[10], M. M. Khaw[11], K-L Tan[11] and H. Akbari[12]
[1]IBM Corp, NY, USA, [2]Nokia, NJ, USA, [3]iNEMI, Shanghai, China, [4]Zestron Europe, Germany, [5]Zestron China, Shanghai, China, [6]Picosun Oy, Espoo, Finland, [7]3M, MN, USA, [8]Georgia Tech, Atlanta, USA, [9]University of Calabria, Italy [10]HP, Bangaluru, India, [11]Keysight, Penang, Malaysia, [12]Schlumberger, TX, USA
pjsingh@us.ibm.com

ABSTRACT
Conformal coatings have traditionally been tested by determining the mean time to failure of conformally coated hardware exposed to corrosive test environments. This test approach has serious shortcomings: The test temperatures are most often too high. At these high temperatures, the conformal coating properties may be quite different from those at the application temperatures. In addition, the times to failure are unacceptably long extending into many months. Overcoming these shortcomings is an iNEMI championed test that involves exposing conformally coated thin films of copper and silver to sulfur vapors at 40-50 ºC in flowers of sulfur (FoS) chamber and using the corrosion rates of the coated metal thin films as a measure of the corrosion protection capabilities of the conformal coatings. The test temperatures are similar to the application temperatures, the test durations are no more than a week and can be conducted under various temperature and humidity conditions. The purpose of this paper was to determine if testing in the industry-standard mixed-flowing gas corrosion chamber would give similar results as those using the FoS chamber. Acrylic, fluorinated acrylate, and atomic layer deposition conformal coatings were tested in three environments: (a) flowers of sulfur (FoS), (b) mixed-flowing gas (MFG), and (c) iodine vapor. The performance of the coatings tested in the FoS and the MFG corrosion chambers were quantitatively similar. The iodine vapor test results were in qualitative agreement with the FoS and MFG test results. In addition, we present early results pointing to the utility of terahertz-frequency imaging as a technique for measuring conformal-coating thickness nondestructively.

INTRODUCTION
Conformal coatings protect coated hardware from the ill effects of moisture, dust, and corrosive gases. With ever-expanding markets for electronic goods, the world over, in environments ranging from benign to very harsh, the need for conformal coatings is ever increasing. Given a wide range of available conformal coatings and given a multitude of hardware on which they need to be applied, it behoves the industry to have standardized means of testing conformal coatings under the application conditions.

Until recently, it was typical to test conformal coatings by applying them to actual hardware and determining the mean time to failure at high temperatures in the neighbourhood of 100 ºC in corrosive, generally flowers of sulfur, environments [1]. This approach suffers two shortcomings: One is that the conformal coating properties at high-test temperatures may be very different from those at the application temperatures; the other is that the test times are too long, extending into many months and sometimes longer. An iNEMI championed novel test approach overcomes these shortcomings by applying the coatings to metal thin films and characterizing the conformal coatings by the degree of corrosion protection they provide the underlying metal thin films [2]. The test temperatures are similar to the application temperatures and the test durations are as short as one week. In the first phase of the iNEMI project that studied this approach, testing was conducted in flowers of sulfur (FoS) chambers. Given that the industry-accepted environment for testing electronic hardware is the mixed-flowing gas (MFG) environment, iNEMI embarked on phase 2 of the project to compare conformal coating test results from testing in the FoS environment to those in the MFG environment.

The iodine vapor test environment was included as the third environment in the project [3].

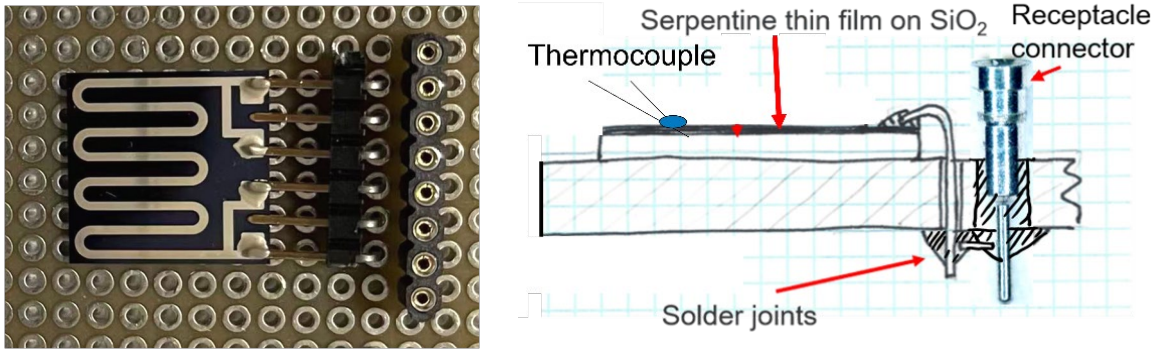

(a) (b)

Figure 1: Thin-film test coupon showing (a) silver serpentine thin film on SiO_2/Si mounted on a circuit board and (b) schematic of cross-section of test coupon showing the way to connect the thin film to the receptacle connector.

This paper compared these three environments in terms of how well they characterize conformal coatings. The conformal coatings chosen for testing provided a range of corrosion protection of the underlying metal thin films: acrylic coating provided moderate corrosion protection; fluorinated acrylate coating provided improved corrosion protection and the atomic layer deposited (ALD) coating provided excellent corrosion protection. The FoS and the MFG tests provided quantitatively similar results on the corrosion protection abilities of the conformal coatings. The iodine vapor test, taking no more than an hour to conduct, provided qualitative corrosion characterization of the coatings that agreed with the results of the FoS and the MFG tests.

In

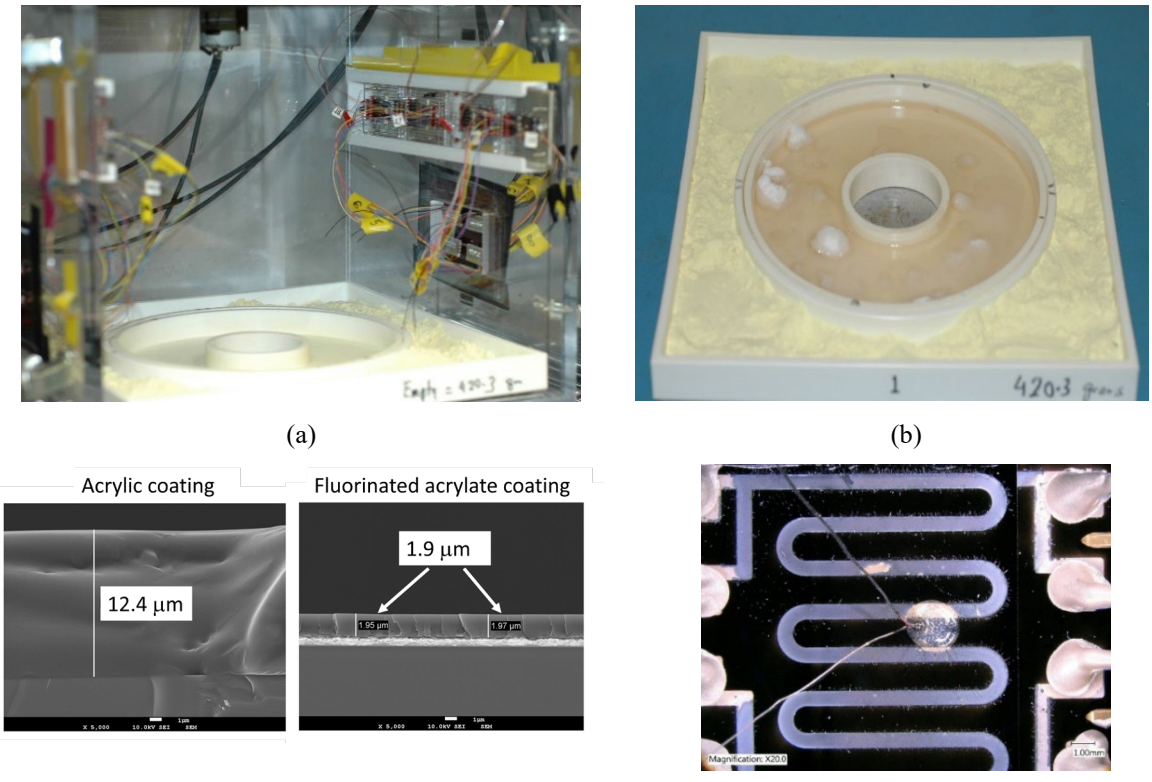

(a) (b)

(c) (d)

Figure 2: Flowers of sulfur (FoS) test setup showing (a) the inside of a FoS chamber with thin films mounted on the chamber walls and sulfur and saturated salt trays on the bottom; (b) the flowers of sulfur tray surrounding the saturated salt solution tray; (c) cross sections of acrylic and fluorinated acylate coatings, and (d) enlarged view of a silver serpentine thin film showing the thermocouple bonded to the surface adjacent to the thin film.

addition to measuring the corrosion rates of conformally coated metal thin films as a means of characterizing

coupon as a serpentine metal thin film deposited on silicon oxide on silicon mounted on a peg printed circuit board with 4-point

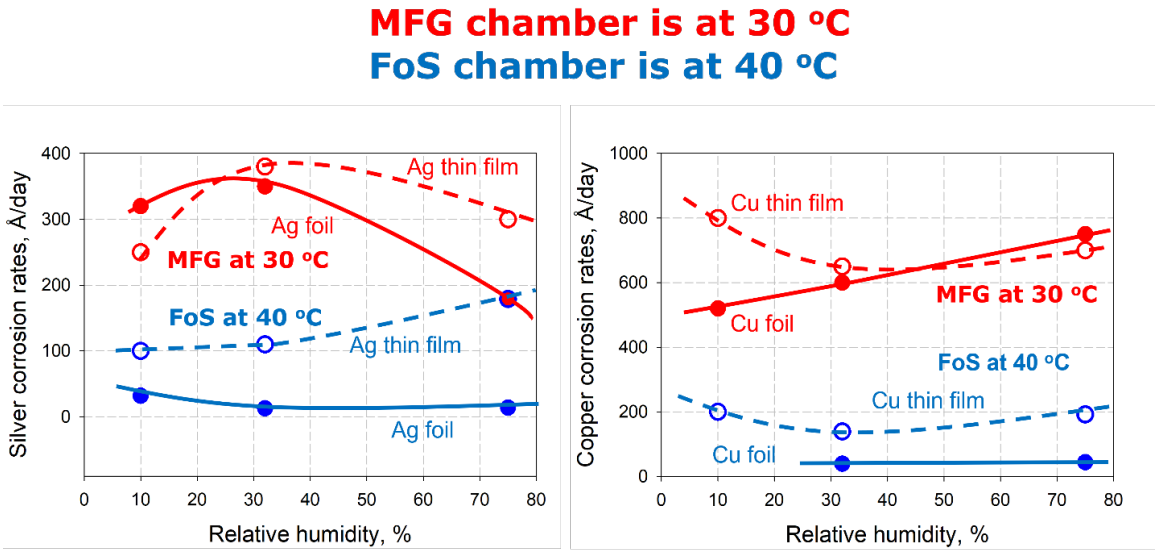

Figure 3: Corrosion rates of bare copper and bare silver thin films and metal foils in MFG and FoS chambers as a function of relative humidity were used to characterize the corrosivity of the chambers

conformal coatings, imaging in the terahertz (THz) band of the electromagnetic spectrum was explored to achieve three-dimensional imaging of the coatings. This technique provides a way to non-destructively measure the conformal-coating thickness and potentially in the future to assess incipient sub-coating corrosion and the condition of the coating itself. Preliminary conformal-coating thickness measurements carried out using this non-destructive THz approach are presented.

TEST METHODS

Conformal coatings were quantitatively characterized by the degree of corrosion protection the coatings provided the underlying, 800-nm thick silver and copper serpentine thin films when exposed to corrosive FoS or MFG environments. **Figure 1** illustrates the thin-film test

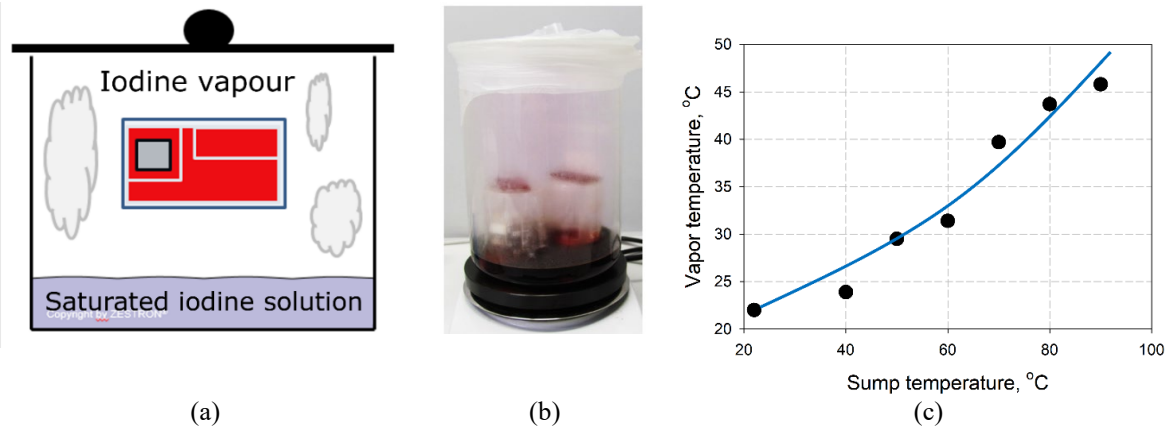

Figure 4: Description of the iodine vapor test: (a) Schematic of the setup; (b) Test chamber; (c) Plot showing that at 70 °C sump temperature, the vapor temperature was 40 °C. The relative humidity in the chamber was 100%.

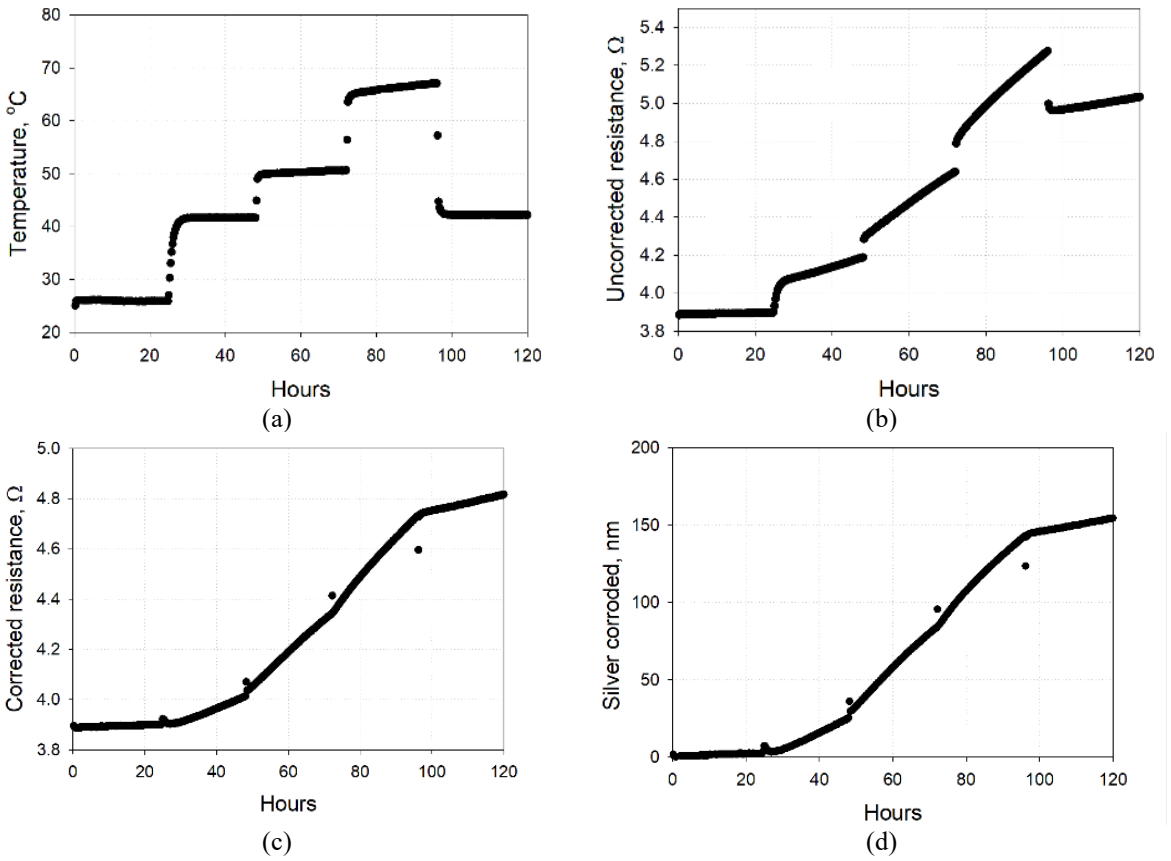

Figure 5: Steps are shown to obtain the thickness of silver corroded as a function of time. This example is for bare silver corroding in 40 ºC, 10% relative humidity environment. The thin-film temperature was stepped to various values by joule heating the film.

resistance measurement connections to a receptable connector. Conformal coatings were characterized by comparing the corrosion rates of the coated thin films to those of uncoated, bare thin films. The corrosion rates of the thin metal films in the FoS and the MFG environments were measured electrically via the rates of change of the resistance of the films. Thin film electrical resistances were measured via the 4-point resistance method in which a known current was pumped through the thin films and the potential drops across them measured. Tests were run in low (10%), medium (32-34%) and high (70-75%) relative humidity environments at 30 ºC in the MFG test chamber and at 40º C in the FoS test chamber. The FoS chamber setup is described in **Figure 2.** The corrosive gas in the FoS chamber was sulfur gas with its concentration kept constant by keeping the chamber temperature constant. The relative humidity in the chamber was kept constant using a saturated salt solution with its deliquescent relative humidity matching the desired relative humidity in the chamber. The temperatures of the thin films and the coatings varied from near the chamber temperature of 40 ºC to as high as 75 ºC using joule

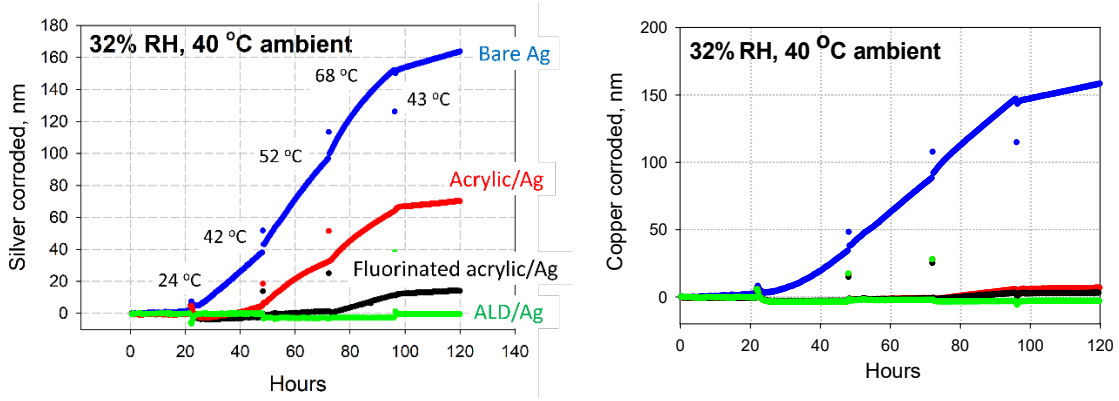

(a) Silver corroded (b)copper corroded

Figure 6: Example of corrosion in FoS chamber at 32% relative humidity and 40 ºC. (a) Thickness of Ag corroded; (b) Thickness of Cu corroded. Note the low corrosion rates of coated Cu compared to coated Ag.

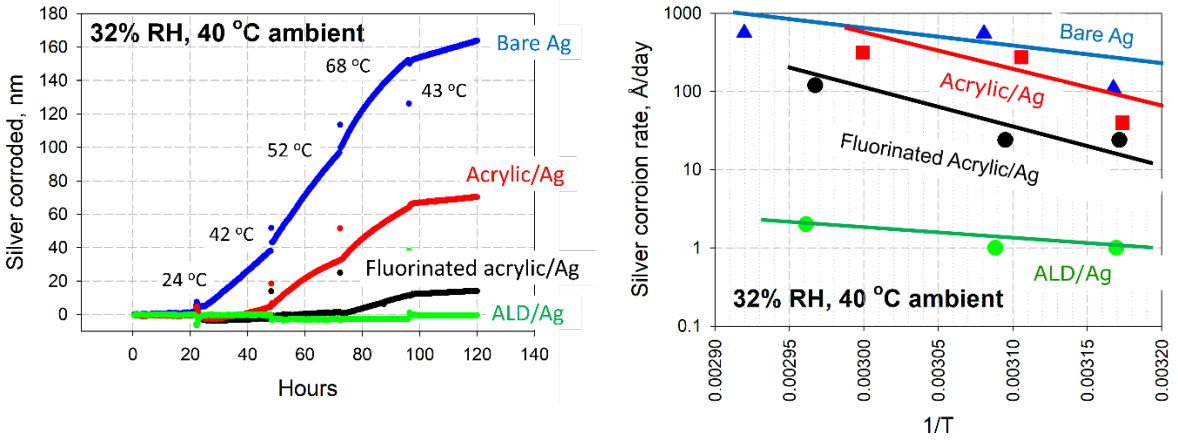

to 16

Figure 7: Example of converting thickness of silver corroded vs time at various temperatures into an Arrhenius pot.

heating. The currents used to measure the film resistances were also used to joule heat the thin films. The temperatures of the coatings were measured using 50-µm diameter T-type thermocouples glued to the coatings. An industry standard MFG chamber was used with the following gas composition: 200 ppb SO_2; 100 ppb H_2S; 200 ppb NO_x and 20 ppb Cl_2. Tests were run at three relative humidity levels of 10, 34, and 70%m all at 30 ºC chamber temperature. In MFG testing also, the conformal coating temperature was raised up to 70 ºC using joule heating by the current that was also used to measure the film resistance.

Corrosion rates of bare copper and bare silver thin films and metal foils were used as a measure of the corrosive nature of the FoS and MFG environments. The thin metal film corrosion rates were measured using the electrical resistance change method. The metal foil corrosion rates were measured either by the mass gain method or by coulometric reduction **[4]**. **Figure 3** summarized these corrosion rates as a function of relative humidity. The corrosion rates of thin metal films are in general higher than those of metal foils because thin films have finer gain size and have higher internal mechanical stresses.

The iodine vapor test involved exposing coated serpentine metal thin films to iodine vapor at 40 ºC and 100% relative humidity for 30 and 60 minutes and optically estimating the extent of the metal film corrosion. The test setup is shown in **Fig. 4a and 4b**. The iodine vapors that come off an iodine saturated aqueous solution at 70 ºC in a sealed container are at 40 ºC, as is evident in the graph of **Fig. 4c.**

In the FoS and the MFG chambers, the extents of the corrosion of bare and of conformally coated copper and silver thin films were measured as a function of time at various temperatures of the conformal coatings. The corrosion rates at various coating temperatures were obtained from the slopes of these plots.

The steps followed to determine the thickness of metal film corroded away as a function of time during five periods, each period lasting one day in the FoS test and 4 hours in the MFG test are shown in **Fig. 5**. The periods were shorter in the MFG test because of the higher corrosion rates in the MFG environment. The example shown in **Fig. 5** is for testing in the FoS environment. During the first period which was the first day in the FoS test, the test chamber was at room temperature. For the remaining four periods, each lasting a day in the FoS test, the chamber temperature was raised to and held constant at 40 ºC. During day 2, the joule heating resulting from 100-mA current raised the film temperature slightly above the ambient to about 42 ºC; during day 3, the 200-mA current raised the film temperature to about 52 ºC; during day 4, the 300-mA current raised the film temperature to about 68 ºC; and during day 5, the 100-mA current lowered the film temperature to about 43 ºC. The jogs in the as-measured resistance plot, shown in **Fig 5b**, we term "uncorrected" resistance, at the instant of change of temperature of the film, were the direct result of the temperature coefficient of electrical resistivity of the metal films. We can compensate for this effect by calculating what would be the film resistance if the film was to be cooled to 40 ºC. This corrected film resistance, with the jogs smoothened out, is plotted in **Fig. 5c**. Knowing that the film thickness is inversely proportional to its electrical resistance, the thickness of metal film corroded away can be calculated.

The above-described procedure was repeated in low, medium, and high relative humidity ambiences at 40 ºC in FoS and at 30 ºC in MFG environments, on copper and silver thin films coated with the three coatings under test along with the uncoated thin films.

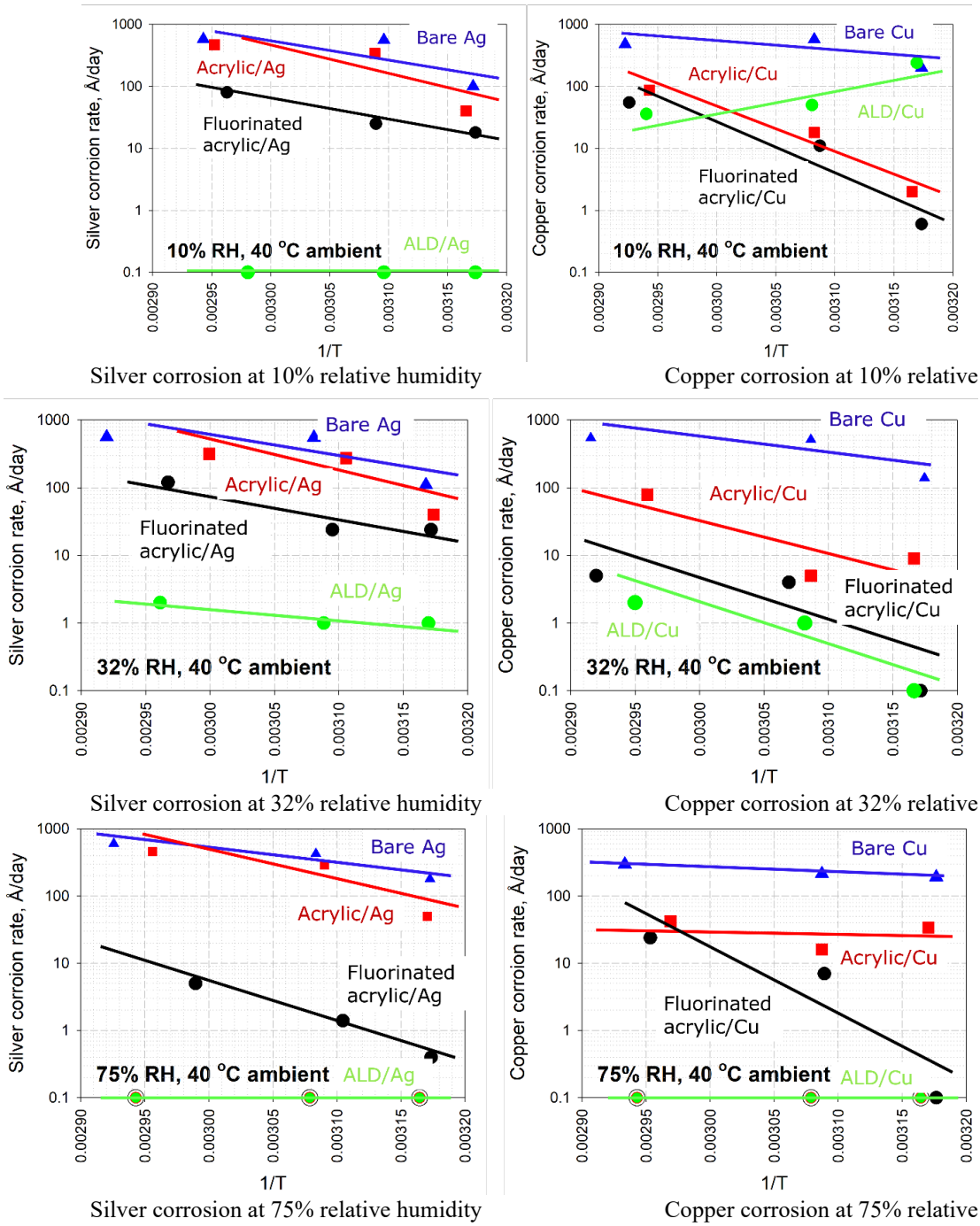

Figure 8: Arrhenius plots of silver and copper corrosion rates in FoS chamber at various relative humidity levels at 40 °C chamber temperature.

Many electrical insulators are transparent to THz frequency (~100 GHz-2 THz) electromagnetic waves, a property that has stimulated interest in THz non-destructive evaluation (NDE) **[5]**. The specific technique employed here is the THz time-of-flight tomography in which a quasi-single-cycle THz pulse is launched onto the test sample. Due to the dielectric discontinuity between the conformal coating and what lies underneath, SiO_2 or metal, the reflected signal is composed of two echoes, one from the air-conformal coating interface and once from the conformal coating-SiO_2 interface. Additional echoes are also seen as discussed later. By measuring the time delay between echoes, which must be extracted using signal-processing techniques due to the temporal overlap of the echoes, and the refractive index of the conformal coating, we obtained the coating thickness. An example is provided below.

The THz experiments were carried out using a pulsed, broadband, THz time-domain system (TPS Spectra 3000, TeraView Ltd, Cambridge, UK). A GaAs photoconductive antenna was excited by an Er- doped fiber laser which emitted sub-100 fs near-infrared pulses at 780 nm at a repetition rate of 100 MHz to produce roughly single circle THz pulses with bandwidth extending from 60 GHz to 3 THz. Balancing the transverse resolution and computational cost, acrylic, fluorinated acrylate, and atomic layer deposition conformal coatings on silver and copper serpentine thin films were raster-scanned by a set of motorized stages moving in the *x*- and *y*- directions with transverse step size 0.1 mm, and each recorded reflected THz pulse contains 4096 data points. The corresponding sampling period T_s was 0.0116 ps. The recorded signal was averaged over 10 shots per pixel to reduce the effect of noise.

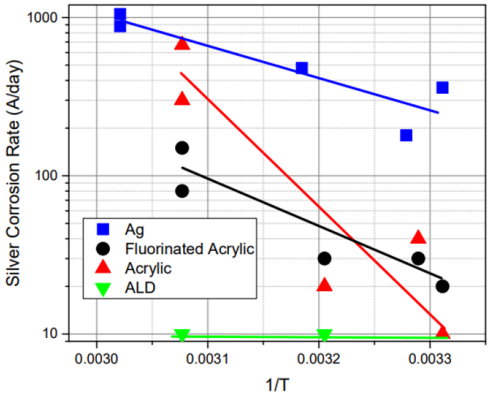

Silver corrosion at 10% relative humidity

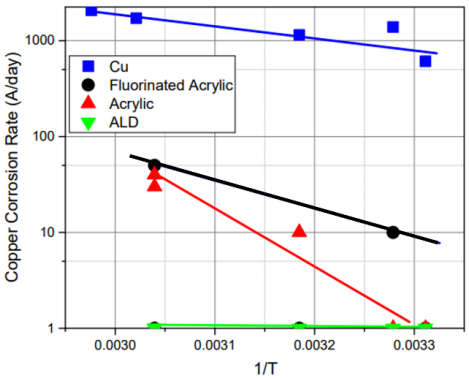

Copper corrosion at 10% relative humidity

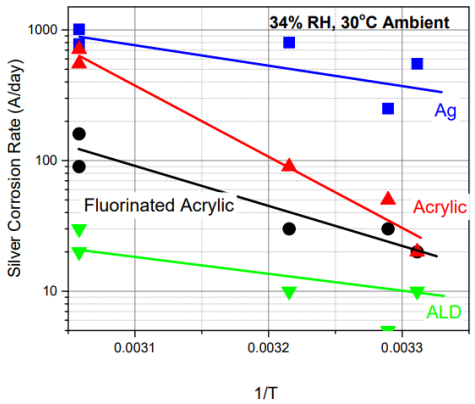

Silver corrosion at 34% relative humidity

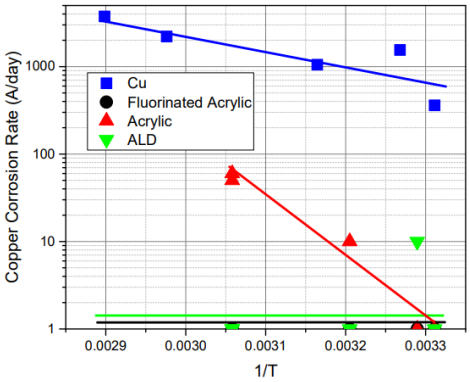

Copper corrosion at 34% relative humidity

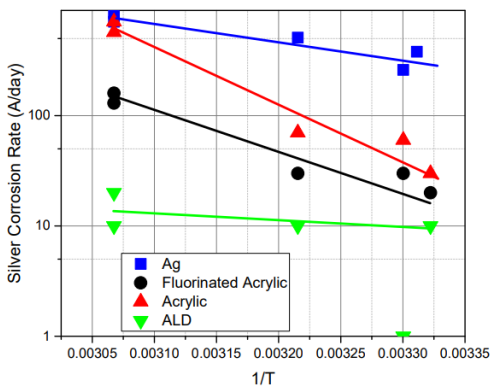

Silver corrosion at 70% relative humidity

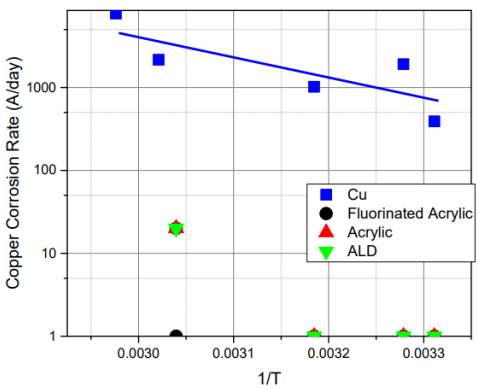

Copper corrosion at 70% relative humidity

Figure 9: Arrhenius plots of silver and copper corrosion rates in MFG chamber at various relative humidity levels at 30 °C chamber temperature.

Table 1: Iodine vapor test results

Coating	Thin film	After 30 minutes in iodine vapors	After 60 minutes in iodine vapors
Acrylic	Ag	Corroded except at the edge where the coating was thicker	Fully corroded
	Cu	No corrosion	Corrosion occurred except in areas of thicker coating
Fluorinated acrylate	Ag	Corroded	Corroded
	Cu	Corrosion started	Corrosion progressed
ALD	Ag	No corrosion	Corrosion started on the edges
	Cu	Slight corrosion	Corrosion proceeded

The specimen, similar to that shown in **Fig. 1** with a Cu serpentine film and an acrylic conformal coating. was subjected to incident THz pulses from the apparatus. The reflected signal was measured, in which were reflected pulses or echoes from the air-conformal coating, conformal-coating/SiO_2 or metal, and conformal coating-PCB interfaces. The sample was rastered in the transverse directions, *x* and *y,* in the THz focus. **Figure 11** shows C-scan images of the specimen in the frequency domain. Based on the broadband nature of a single-cycle THz pulse, THz multispectral images were obtained by taking the Fourier transform of the reflected signal $r(t)$ at each pixel and integrating the magnitude of the frequency components within various bands. We plotted the THz data in a frequency window at a given pixel by

$$E' = \int_{f_l}^{f_h} |FFT(r(t))| dv \qquad (1).$$

where f_l and f_h are the limits of the window. The effective bandwidth of the THz pulse was divided into six bands, each of width 0.5 THz, as shown in **Fig. 11a**, to obtain better resolution in the higher-frequency bands.

RESULTS AND DISCUSSION

An example of coated and uncoated silver and copper thin films corrosion in the FoS chamber is shown in **Fig. 6** for 32% relative humidity and 40 °C test run. The plots of the thickness of silver and copper corroded versus time have almost no jogs associated with temperature changes, indicating well-chosen values of the silver and copper coefficients of electrical resistivities. Anyway, it was discovered that the selected coefficients of resistivity values had little effect on the calculated corrosion rates. From the slopes of a metal corroded plot (**Fig 7a**) at various temperatures, the corrosion rates can be obtained and plotted in an Arrhenius fashion as shown in **Fig. 7b**.

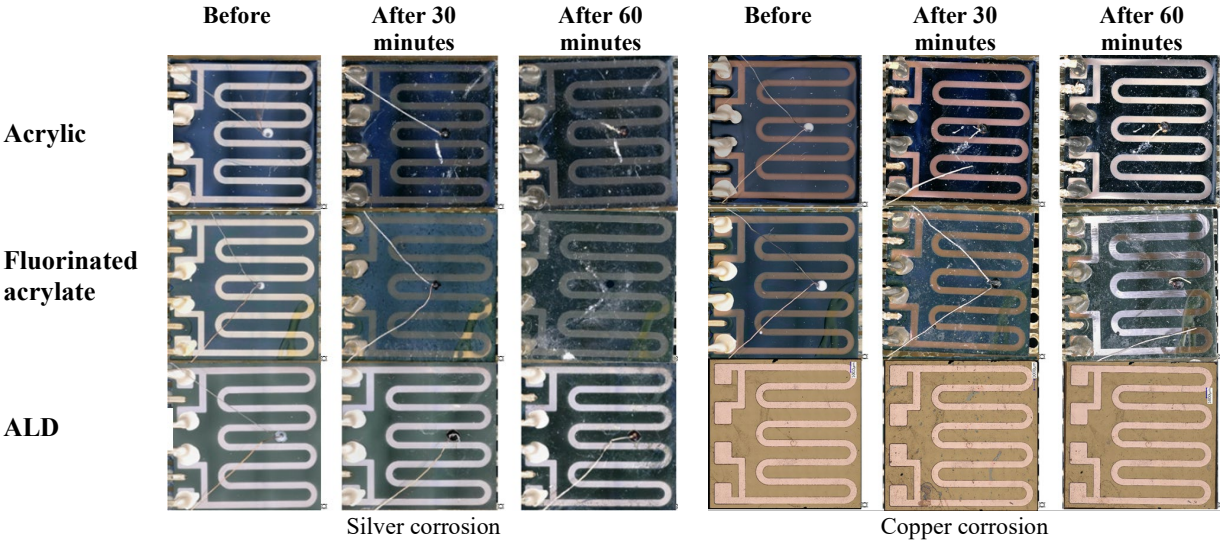

Figure 10: Visual inspection of the coated thin films subjected to iodine vapors for 30 and 60 minutes under a low magnification microscope indicates that the thin films under the acrylic coatings corroded the most, the fluorinated acrylate coated thin films corroded less and the ALD coated thin films corroded the least. The ALD-coated thin copper films look different because the thin films were precleaned before the deposition of the ALD coating.

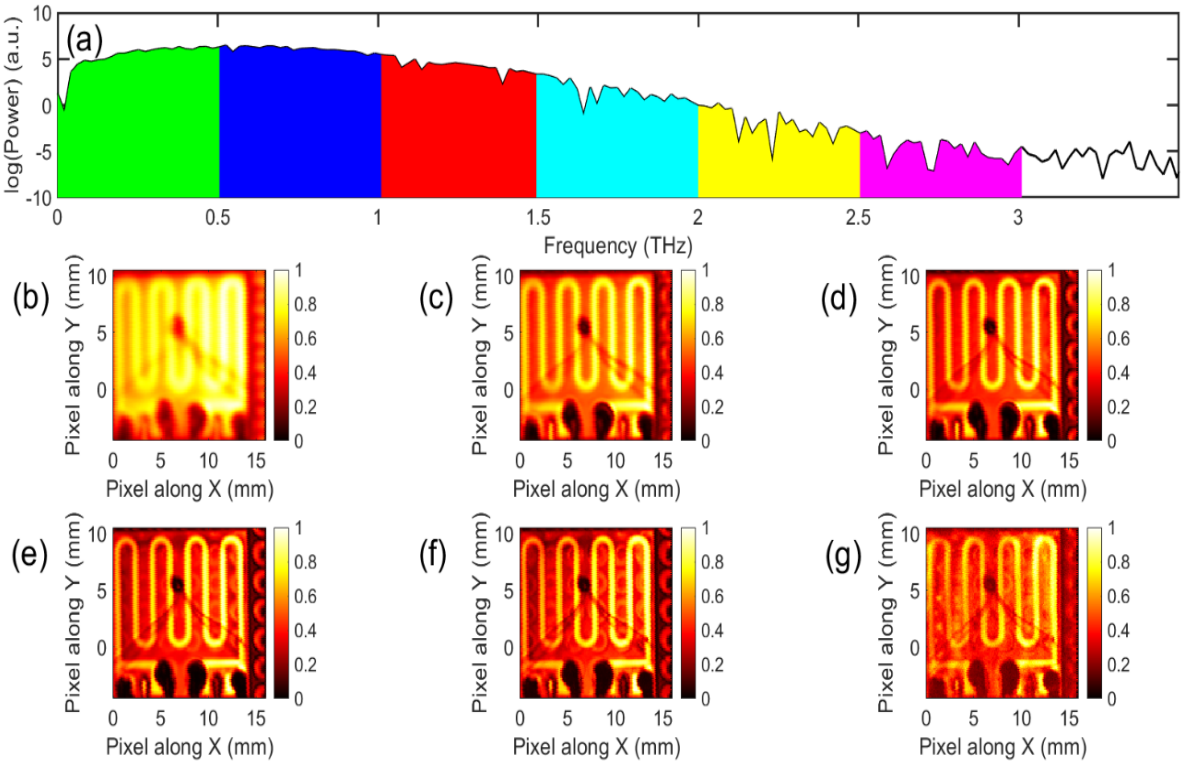

Figure 11: (a). Power spectrum of the reference THz pulse produced by our THz system. The full spectrum of a broadband THz pulse [0 THz, 3 THz] is divided into six frequency bands of 0.5 THz widths. THz multispectral images of acrylic-coated copper serpentine thin film obtained based on the components in frequency bands within (b) [0, 0.5 THz], (c) [0.5 THz, 1 THz], (d) [1 THz, 1.5 THz], (e) [1.5 THz, 2 THz], (f) [2 THz, 2.5 THz], (g) [2.5 THz, 3.0 THz].

The corrosion rates of uncoated and coated copper and silver thin firms in 10, 32, and 75% relative humidity FoS environments are summarized in the Arrhenius plots of **Figure 8**. Notice that in general the corrosion rates of coated copper thin films are less than those of coated silver thin films indicating that copper is better protected from corrosion by the conformal coatings.

The corrosion rates of uncoated and coated copper and silver thin firms in 10, 34, and 70% relative humidity MFG environments are summarized in the Arrhenius plots of **Figure 9**. Notice that, in this case too, in general, the corrosion rates of coated copper thin films are less than those of coated silver tin films indicating that copper is better protected from corrosion by the conformal coatings.

As expected by the more corrosive environment in the MFG chamber, the corrosion rates of uncoated and coated thin films were in general higher in the MFG chamber compared to in the FoS chamber; though the results from the coatings tested in the two environments trend in a similar manner: The ALD coating provided the best corrosion protection to the coated metal film; the fluorinated acrylate the next best protection and the acrylic coating provided lesser protection.

The relatively linear nature of the Arrhenius plots of **Figs. 8 and 9** indicate that the transport mechanism of corrosive chemical species through the conformal coatings remains the same over the 40 to 75 ºC range of temperature employed in this study. In both the FoS and the MFG tests, the temperature had a strong degrading effect on the acrylic and the fluorinated acrylate coatings. The corrosion rates of the ALD coatings were too low to observe any temperature effects.

The iodine vapor test results are shown in **Fig. 10** for silver and copper thin films and are tabulated in **Table 1**. Silver and copper thin films under the ALD coatings corroded the least; the films corroded a little more under the fluorinated acrylate coatings and the most under the acrylic coatings, in agreement with the test results in the FoS and the MFG chambers.

We now turn to the results of THz imaging. THz

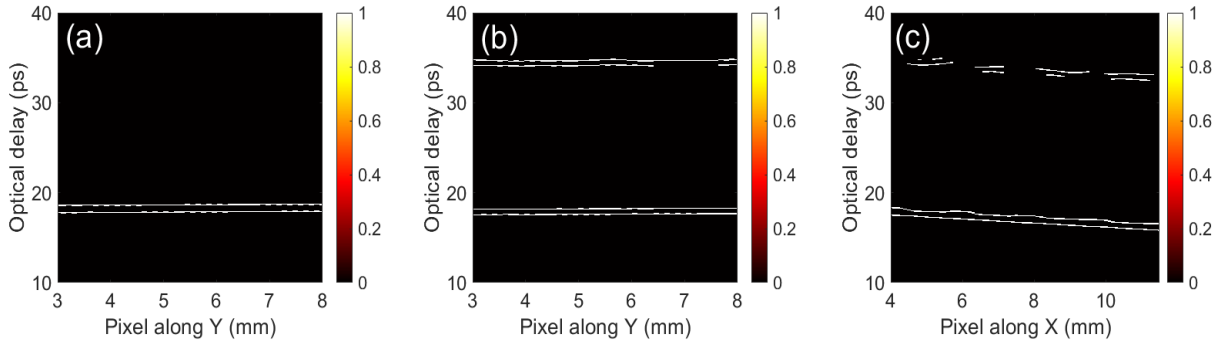

Figure 12: Binary THz B-scans based sparsity-based reconstruction of impulse response function in reflection along cross-sections (a) x = 2.3 mm (on serpentine film), (b) x=3.3 mm (between serpentine film), and (c) y=8 mm (across serpentine film) in Fig. 10(b).

multispectral C-scans of the test sample in the six frequency bands are plotted in **Fig. 11b-g.** Images in the low-frequency band are dominated by noise, and the serpentine film becomes clearer as the frequency increases as higher frequency components correspond to shorter wavelengths. In the highest band shown, noise causes the image, though still sharp, to fade.

We proceeded with the THz time-of-flight tomography experiments, also in reflection, to obtain the conformal-coating thickness. Because the coating was optically thin ($\sim\lambda$ near 1 THz in the medium), successive THz echoes overlapped and were not visually evident in the reflected signal. We, therefore, employed sparsity-based deconvolution [6] to reconstruct the impulse response function and obtain the coating thickness.

The impulse-response function that determines the reflected signal consists mainly of a baseline at zero with a sparse sequence of sharp peaks associated with reflections from the interfaces. By performing a peak-detection on the reconstructed impulse response function, both positive and negative peaks. and setting a threshold, binary B-scans (cross-section through the sample) are plotted. Peaks of amplitude greater than the threshold are assigned a value of "1", while all other time points are "0".

The binary THz B-scans at (a) x = 2.3 mm (section along serpentine film), (b) x=3.3 mm (the section between serpentine film), and (c) y=8 mm (section across serpentine film), in **Fig. 11** are shown in **Fig. 12.** The THz signal is incident from the bottom of the figures (conformal-coating side); the top side is the SiO_2. In (b), we see two peaks near the time delay of 18 ps corresponding to the air/acrylic and the acrylic/SiO_2 interfaces. The two peaks near 35 ps correspond to the SiO_2/epoxy and epoxy/PCB interfaces. In (a), however, the serpentine film reflects most of the incident THz radiation casting a shadow below, accounting for the absence of features associated with the underlying SiO_2/epoxy and epoxy/PCB interfaces. In (c) we see the alternation of the shadow with the underlying features as the beam is rastered across the serpentine film.

The acrylic thickness distribution is obtained by multiplying the relative time delay Δt between the two peaks at ~18 ps and multiplying by c/n, where c is the speed of light and n = 1.62 is the refractive index of acrylic near 1 THz [7]. The acrylic thickness corresponding to **Fig. 12** is shown in **Fig. 13**. **Figures 13** (a) and (b) show the relatively uniform conformal-coating thickness of (a) 73.8 ± 0.8 µm, and (b) 54.7 ± 1.4 µm. Discrepancies between the calculated conformal-coating thickness based on THz results and the nominal value might originate from exposure to 32 % relative humidity in an FoS environment at 40°C for 5 days as this likely alters n from its nominal

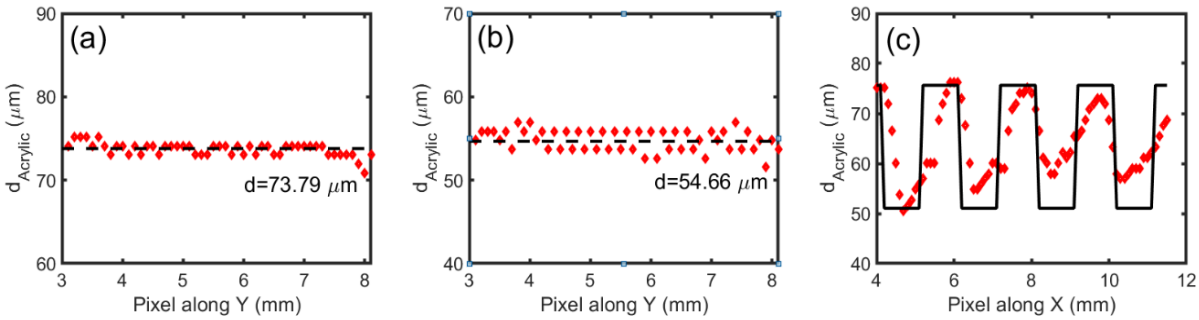

Figure 13: Thickness distribution of acrylic-coated Cu serpentine thin film along (a) x = 2.3 mm (on serpentine film), (b) x=3.3 mm (between serpentine film), and (c) y=8 mm (across serpentine film) as in Fig. 11. Square wave in (c) is a guide to the eye.

value. We also note that the acrylic thickness on top of the serpentine appears to be thicker than between the serpentine film, though there might also be an aging-induced transverse variation of *n*.

CONCLUSIONS

The flowers of sulfur (FoS) and the mixed-flowing gas (MFG) test results were in quantitative agreement in their characterization of the corrosion protection provided by the acrylic, the fluorinated acrylate, and the atomic layer deposited coatings. The coatings tested provided much better corrosion protection to the underlying copper than to silver, probably because of the better adhesion of the coatings to copper.

The FoS chamber is of simple construction, and easy to operate **[8]**. It is a couple of orders of magnitude less expensive to own and operate compared to the MFG chamber. This study demonstrated that the FoS chamber is as effective an environment as the industry standard MFG chamber in testing conformal coatings. The iodine vapor test can be done in an hour. Its characterization of conformal coatings is in qualitative agreement with the results from the FoS and the MFG tests.

The non-destructive THz thickness measurements of the acrylic conformal coating were carried out. Film thickness measured was in reasonable agreement with the thickness obtained by cross sectioning means; however, the small discrepancy might be due to aging effects of the film. The THz measurements suggest the acrylic coating is somewhat thicker on the Cu serpentine films than in the space between them., an observation yet to be independently verified. Possible future research effort may focus on detecting incipient sub-coating corrosion and chemical degradation of the conformal coating itself.

REFERENCES

[1] M. Cole, J. Porter, J. Wertz, M. Coq, J. Wilcox, and M. Meilunas, "Conformal coatings in preventing resistor silver sulfide corrosion," Proceedings of SMTA Int'l, Rosemont, IL, USA, 25-29 Sept 2016.

[2] P. Singh, L. Palmer, and M. Gaynes, "Conformal coating characterization using stacked silver thin films," 2020 SMTA Int'l Pan Pacific Symposium, Hi, USA, 10-13 Feb 2020.

[3] M. R. Meier, and H. Schweigart, "Quality test for potting materials regarding susceptibility to harmful gases and humidity," EBL 2020 - Elektronische Baugruppen und Leiterplatten conference, Germany, 18-19 Feb 2020.

[4] S. J. Krumbein, B. Newell, and V. Pascucci, "Monitoring environmental tests by coulometric reduction of metallic control samples," Journal of Testing and Evaluation, ASTM 1989.

[5] J. P. Guillet, H. Recur, L. Frederique, B. Bousquet, L. Canioni, I. Manek-Hönninger, P. Desbarats, and P. Mounaix, "Review of Terahertz Tomography Techniques." *J Infrared Milli Terahz Waves*, vol. 35, pp. 382–411, 2014. https://doi.org/10.1007/s10762-014-0057-0

[6] J. Dong, X. Wu, A. Locquet and D. S. Citrin, "Terahertz Superresolution Stratigraphic Characterization of Multilayered Structures Using Sparse Deconvolution," IEEE Transactions on Terahertz Science and Technology, vol. 7, no. 3, pp. 260-267, May 2017.

[7] M. Zhai, A. Locquet, and D. S. Citrin, "Pulsed THz imaging for thickness characterization of plastic sheets," NDT&E International, vol. 116, p. 102338, Dec 2020.

[8] P. Singh, H. Fu, C. Xu, S. Lee, L. Palmer, D. Lee, K. Guo, J. Liu, "iNEMI general purpose FoS corrosion chamber," IPC APEX Expo, San Diego, CA, 2019